

1 **Role of non-coding RNA hsa\_circ\_0001495 in 16HBE cellular**  
2 **inflammation induced by PM<sub>2.5</sub> and O<sub>3</sub> combined exposure**

3 HongJie Wang<sup>a,b,1</sup>, Yi Tan<sup>a,1</sup>, CaiXia Li<sup>c</sup>, WenJia Jin<sup>c</sup>, Ying Yu<sup>b</sup>, Xuan Mu<sup>b</sup>, XiaoWu  
4 Peng<sup>a,\*</sup>

5 <sup>a</sup> *State Environmental Protection Key Laboratory of Environmental Pollution Health Risk*  
6 *Assessment, South China Institute of Environmental Sciences. Ministry of Ecology and*  
7 *Environment, Guangzhou 510535, China*

8 <sup>b</sup> *School of Public Health, China Medical University, Shenyang 110122, China*

9 <sup>c</sup> *School of Public Health, Guangxi Medical University, Nanning 530021, China*

10 *\* Author to whom correspondence should be addressed*

11 **Abstract**

12 **Background:** PM<sub>2.5</sub> and O<sub>3</sub> are the main air pollutants in China, and  
13 inflammation of the respiratory system is one of their main toxic effects. Cyclic RNAs  
14 are involved in many pathophysiological processes, but their relationship to the  
15 combined exposure to PM<sub>2.5</sub> and O<sub>3</sub> has not yet been investigated.

16 **Objective:** To elucidate the biological function played by hsa\_circ\_0001495 in  
17 the induction of 16HBE cellular inflammation by combined exposure to PM<sub>2.5</sub> and O<sub>3</sub>.

18 **Method:** Detection of cell survival after 24h exposure of 16HBE cells to a  
19 combination of PM<sub>2.5</sub> and O<sub>3</sub> by CCK8. RT-qPCR and ELISA were used to detect  
20 inflammatory factors in 16HBE cells after co-exposing to PM<sub>2.5</sub> and O<sub>3</sub>. CircRNA  
21 was screened using high throughput sequencing and bioinformatics analysis  
22 approaches. RNaseR experiments were carried out to verify the circular RNA  
23 properties of the circRNAs. Cytoplasmic-nuclear subcellular localisation assays and  
24 fish assays were used to verify the distribution of circRNAs in the nucleus versus the  
25 cytoplasm of the cell. To validate functions related with circRNA, RT-qPCR and  
26 ELISA were employed.

27 **Result:** Combined exposure to PM<sub>2.5</sub> and O<sub>3</sub> resulted in decreased cell  
28 viability. Combined exposure to PM<sub>2.5</sub> and O<sub>3</sub> resulted in 16HBE inflammation. High  
29 throughput sequencing and RT-qPCR results showed that the expression of  
30 hsa\_circ\_0001495 was significantly downregulated in 16HBE exposed to PM<sub>2.5</sub> and  
31 O<sub>3</sub> in combination. Hsa\_circ\_0001495 is not easily digested by RNaseR enzymes and  
32 has the properties of a circular RNA. Hsa\_circ\_0001495 is expressed in the cytoplasm  
33 as well as in the nucleus, but its distribution is predominantly in the cytoplasm.

34 **Conclusion:** In 16HBE cells, combined exposure to PM<sub>2.5</sub> and O<sub>3</sub> can induce an  
35 inflammatory response. hsa\_circ\_0001495 plays an inhibitory role in the inflammatory  
36 response of 16HBE cells that can be induced by combined exposure to PM<sub>2.5</sub> and O<sub>3</sub>.

37 Key words: PM<sub>2.5</sub>; O<sub>3</sub>; compound exposure; inflammation; 16HBE ; circRNA

38

39

## 1.Introduction

40 PM<sub>2.5</sub> is mainly generated through natural pathways such as volcanic eruptions  
41 and forest fires <sup>[1]</sup> and anthropogenic pathways such as fossil fuel combustion due to  
42 human production and living <sup>[2]</sup> Numerous epidemiological studies have shown <sup>[3]</sup> that  
43 living in an environment with high concentrations of PM<sub>2.5</sub> for a long period of time  
44 can significantly increase the incidence of disease and mortality in the population,  
45 such as respiratory and cardiovascular diseases and many other diseases. It has been  
46 reported <sup>[4]</sup> that for every 10 ppb (21.44 µg/m<sup>3</sup>) increase in O<sub>3</sub> concentration, the  
47 respiratory mortality rate increases by 0.64% (95% PI: 0.31%-0.98%). The  
48 association between atmospheric O<sub>3</sub> pollution and increased risk of respiratory disease  
49 is well established<sup>[5, 6]</sup>, and inhalation of O<sub>3</sub> may damage lung epithelial cells <sup>[7,</sup>  
50 <sup>8]</sup>. Wong <sup>[9]</sup> et al. found that the combined exposure to ultrafine particles and O<sub>3</sub>  
51 increased the extent of lung damage, with severe damage to both the large airways  
52 and the small airways, and was not a additive effect of a single pollutant exposure

53 PM<sub>2.5</sub> and O<sub>3</sub> and the inflammatory effect on the respiratory system is one of the main  
54 toxic effects, and there is a synergistic effect between the two. A large number of  
55 studies have shown that PM<sub>2.5</sub> and O<sub>3</sub> and the mechanism of respiratory system  
56 damage caused by the inflammatory response is considered to be the basic pathogenic  
57 mechanism. Happono<sup>[10]</sup> and other studies have found that PM<sub>2.5</sub> can directly stimulate  
58 alveolar macrophages (AMs) to secrete a large number of pro-inflammatory cytokines,  
59 chemokines, leading to diffuse inflammation in the lungs. It was found<sup>[11]</sup> that IL-1 $\alpha$   
60 released from O<sub>3</sub>-induced tissue damage and inflammation is mediated by MyD88  
61 signalling in epithelial cells. In recent years, with the rapid development of biological  
62 science theories and technologies, circular RNA (circRNA) has received keen  
63 attention from research scholars. circRNA is a closed-loop non-coding RNA  
64 covalently linked at the 3' and 5' ends produced in the process of reverse splicing, and  
65 it has a high degree of tissue-expression specificity in the eukaryotic transcriptome<sup>[12]</sup>.  
66 In this experimental study, we found that an abnormally low expression of  
67 has\_circ\_0007766 occurred after compound exposure of human bronchial epithelial  
68 cells (16HBE) stained with PM<sub>2.5</sub> (100  $\mu$ g/ml) + O<sub>3</sub> (300ppb,2h). This study was  
69 designed to explore the inflammatory response induced by compound exposure of  
70 16HBE cells with PM<sub>2.5</sub> and O<sub>3</sub> and the has\_circ\_0007766 in this process to provide a  
71 scientific basis for PM<sub>2.5</sub>-induced respiratory diseases.

72

## 73 **2. Materials and methods**

### 74 **2.1 Cell and cell culture**

75 Human bronchial epithelial cells (16HBE) were obtained from the group of Wu  
76 Jianjun from Guangzhou Medical University, China. 16HBE cells were grown in  
77 MEM complete medium (Cienry, China), which consisted of 1%  
78 penicillin/streptomycin (gibico, USA), 5% foetal bovine serum (Four Seasons Green,  
79 China), and 94% MEM basal medium, and cultured at air-liquid interface with

80 Transwell (Corning, USA) at a temperature of 37°C and CO<sub>2</sub> concentration of 5%.  
81 The cells were cultured at the air-liquid interface using Transwell (Corning, USA) at a  
82 temperature of 37°C and a concentration of 5% carbon dioxide.

## 83 **2.2 Preparation of PM<sub>2.5</sub> and O<sub>3</sub> subjects**

84 From March to November 2021, On the roof of an office building (Huangpu  
85 District, Guangzhou, Guangdong) collecting PM<sub>2.5</sub>. The TH1000C large flow sampler  
86 (Wuhan Tianhong, China) was used to collect PM<sub>2.5</sub> with a sample flow of 1.05  
87 m<sup>3</sup>/min and 72h of continuous sampling. O<sub>3</sub> occurs in ozone calibrators (2Btech, USA).

## 88 **2.3 Cellular contamination**

89 The Cloud System Particulate Dyeing Instrument (VOTROCELL CLOUD12,  
90 Germany) as well as the Continuous Fluid External Exposure System (VOTROCELL  
91 12/12, Germany) were used to compound exposure to PM<sub>2.5</sub> and O<sub>3</sub> in 16HBE cells.

## 92 **2.4 Cell Counting Kit-8 Assay**

93 The Cell Counting Kit-8 (CCK-8) (Biosharp, China) was used to measure cell  
94 viability. Human bronchial epithelial cells were cultured in a 12-well Transwell and  
95 treated with PM<sub>2.5</sub> and O<sub>3</sub> for 24 hours, and the grouping of contamination was  
96 divided into 0, PM<sub>2.5</sub> (100 µg/ml), PM<sub>2.5</sub> (100 µg/ml) + O<sub>3</sub> (300ppb, 2h), PM<sub>2.5</sub>  
97 concentrations were selected based on previous experiments conducted by the group  
98 and relevant literature. <sup>[13-15]</sup>, and the concentration of O<sub>3</sub> toxicity was taken from the  
99 literature <sup>[16-18]</sup>, and the experiment was carried out in three biological replicates. After  
100 24h of contamination, the cells were washed with PBS, added with CCK8 reagent  
101 mixture, and incubated for 1h, protected from light. Absorbance at 450nm was  
102 measured by microplate reader (BioTek Synergy HT, USA). Cell viability was  
103 calculated according to the instructions.

## 104 **2.5 RT-qPCR analysis**

105 The experimental groupings were: 0, PM<sub>2.5</sub> (100 µg/ml), PM<sub>2.5</sub> (100 µg/ml) +  
106 O<sub>3</sub> (300ppb, 2h). Human bronchial epithelial cells were inoculated into 12-well

107 Transwell cell chambers at  $1.5 \times 10^5$  cells/well and cultured for 24h after exposure to a  
108 combination of PM<sub>2.5</sub> and O<sub>3</sub>. SevenFast® Total RNA Extraction Kit(SEVEV,China)  
109 was used to extract total cellular RNA. Evo M-MLV RT Kit with gDNA Clean for  
110 qPCR II (Accurate Biology,China )was used to reverse transcribe the total RNA. qRT-  
111 PCR was conducted using SYBR®Green Pro Tap HS(Accurate Biology,China)and  
112 detected by Step One Plus(Applied Biosystems,USA). Relative gene expression level  
113 =  $2^{-\Delta\Delta Ct}$ .ACTB ( $\beta$ -actin) was used as an internal reference gene for correction of  
114 relative gene expression. The primers are shown in Table S1.

## 115 **2.5 Enzyme-linked immunosorbent assay**

116 The experimental groupings were: 0, PM<sub>2.5</sub> (100  $\mu$ g/ml), PM<sub>2.5</sub> (100  $\mu$ g/ml) + O<sub>3</sub>  
117 (300ppb,2h). Human bronchial epithelial cells were inoculated into 12-well Transwell  
118 cell chambers at  $1.5 \times 10^5$  cells/well and cultured for 24h after exposure to a  
119 combination of PM<sub>2.5</sub> and O<sub>3</sub>. ELISA kits were used to detect the levels of cellular  
120 inflammatory factors IL-8, IL-1 $\beta$  protein exp(Jiubang,China)ression. The OD value of  
121 the measured standard was taken as the horizontal coordinate, and the concentration  
122 value of the standard (the concentration of the standard was 80, 40, 20, 10, 5, 2.5  
123 pg/mL in order) was taken as the vertical coordinate, and the standard curve was  
124 plotted by Excel software, and a linear regression equation was obtained, and the OD  
125 value of the samples was substituted into the equation, and the concentration of the  
126 samples was calculated.

## 127 **2.5 High-throughput sequencing and data analysis**

128 Samples of 16HBE were collected for high-throughput sequencing after  
129 exposure to PM<sub>2.5</sub>+O<sub>3</sub> (0, PM<sub>2.5</sub>+O<sub>3</sub>) for 24 hours.The technology has been done at  
130 Shanghai Kangcheng Biotechnology Co., Ltd.

## 131 **2.6 RNase R experiment**

132 Cells were inoculated into 12-well Transwell cell chambers at  $1.5 \times 10^5$  cells/well

133 and placed in the incubator for 24 h. Total cell RNA was extracted after the cell fusion  
134 rate reached 70%-80%. Then the extracted cell RNA was subjected to the experiment  
135 according to the instructions of the de-novo enzyme experiment. Experimental  
136 grouping: RNase R+ group (RNase R enzyme treatment) and RNase R- group (no  
137 RNase R enzyme treatment), 4U of RNase R reagent was added to 2.4 µg of total  
138 RNA (RNase R+ group), and after incubation at 37°C for 10 min, reverse  
139 transcription as well as qRT-PCR experiments were performed to detect hsa\_circ\_  
140 0007766 and the expression of the internal reference ACTB ( $2^{-\Delta\Delta Ct}$ ). The internal  
141 reference ACTB in the RNase R-group was used for subsequent calculations. RNase  
142 R experiment were carried out according to the RNase R instructions (Guangzhou  
143 Genesee Biological Technology Co., Ltd, China).

## 144 **2.7 Nucleocytoplasmic separation experiment**

145 Cells were inoculated with  $10^6$  cells/well in a 10 cm dish and placed in an  
146 incubator for 24 h. After the cell fusion rate reached 70%-80%, nucleoplasmic  
147 separation experiments were carried out using the Invitrogen PARIS™ am1921 kit  
148 (Invitrogen AM1921, USA), and the nuclei and cytoplasm were extracted. qRT-PCR  
149 experiments were carried out to detect the expression ( $2^{-\Delta\Delta Ct}$ ) of the  
150 hsa\_circ\_0007766 and the internal reference genes (ACTB, U6), and the primer  
151 sequences are shown in Table S2.

## 152 **2.8 Fluorescence in situ hybridization**

153 The FISH procedure followed the RNA FISH kit instructions (GenePharma,  
154 China). Finally, cells were examined with IX71 Inverted Research System  
155 Microscope (Olympus, Japan). The FISH probe were designed by the Suzhou  
156 GenePharma Co., Ltd. The probe sequences are shown in Table S2.

## 157 **2.9 Transient transfection of cyclic RNA**

### 158 **2.9.1 Transfection efficiency assay**

159 The 16HBE cells were inoculated in 6-well plates at a density of  $4.5 \times 10^5$  cells/well.  
160 80%-90% cell density was achieved after 24h, and the next experiment could be  
161 carried out. The experimental groups were as follows: hsa\_circ\_0007766 group  
162 (hsa\_circ\_0007766 plasmid), negative transfection control group (NC), MOCK group  
163 (transfection reagent control group). Transfection complexes were prepared: part A:  
164 121  $\mu$ l Opti-MEM medium + 4  $\mu$ l lipofectamine 3000; part B: 112.23  $\mu$ l Opti-MEM  
165 medium + 6.77  $\mu$ l overexpression solution + 5  $\mu$ l P3000, part C: 114  $\mu$ l Opti-MEM  
166 medium + 6  $\mu$ l NC solution + 5  $\mu$ l P3000; Part D: 120  $\mu$ l Opti-MEM medium + 5  $\mu$ l  
167 P3000. The transfection complex was prepared by mixing A and B, A and C, A and D  
168 in the ratio of 1:1, and placed at room temperature for 20 min, and then the  
169 transfection complexes were added into cell culture plates according to the  
170 experimental grouping, and the amount of solution per well was 250  $\mu$ l of transfection  
171 complex + 1.75 ml Opti-MEM culture medium. After 5h of culture, the old medium  
172 was aspirated, the cells were rinsed using PBS buffer to remove the residual liquid,  
173 and then 2ml of MEM complete medium was added to culture the culture for 24h,  
174 then the cellular RNA was extracted, and the changes of hsa\_circ\_0007766 level were  
175 detected by qRT-PCR. The overexpression sequence was designed and synthesised by  
176 Suzhou Gemma.

### 177 2.9.2 Validation of cyclic RNA function

178 Experimental grouping: 16HBE cells were divided into four groups, NC group  
179 (overexpression of plasmid-negative transfection sequence), hsa\_circ\_0007766 group  
180 (overexpression of plasmid by hsa\_circ\_0007766), NC+ PM<sub>2.5</sub> (100  $\mu$ g/ml) + O<sub>3</sub>  
181 (300ppb, 2h) group (overexpression of plasmid-negative transfection sequence +PM<sub>2.5</sub>  
182 (100  $\mu$ g/ml) + O<sub>3</sub> (300ppb, 2h)), hsa\_circ\_0007766+ PM<sub>2.5</sub> (100  $\mu$ g/ml) + O<sub>3</sub> (300ppb,  
183 2h) group (hsa\_circ\_0007766 overexpression plasmid +PM<sub>2.5</sub>(100 $\mu$ g/ml)+O<sub>3</sub>(300ppb,  
184 2h)), the transfection complex was prepared as in 2.9.1, according to the experimental

185 grouping, the transfection complex was added to the upper chamber of the Transwell  
186 with the Opti-MEM medium, and the lower chamber was added with 1.5 ml of the  
187 Opti-MEM medium, and then the waste liquid was discarded and washed with PBS  
188 for two times, and then replaced with the serum free medium of the MEM. Then  
189 PM<sub>2.5</sub>+O<sub>3</sub> staining, after 24h of culture, the cell RNA was extracted, and then by  
190 qRT-PCR (reaction system and conditions are the same as 1.5.1), the gene  
191 expression= $2^{-\Delta\Delta Ct}$ ; ELISA detected the changes in the transcription and protein  
192 levels of the inflammatory factors IL-1 $\beta$  and IL-8 (the results of the experiment were  
193 based on the OD value of the measured standard as the horizontal coordinate, the  
194 standard concentration value (the concentration of the standard in the order of: 80, 40,  
195 20, 10, 5, 2.5 pg/mL) as the vertical coordinate, the standard curve was drawn by  
196 Excel software, and the linear regression equation was obtained, the OD value of the  
197 sample was substituted into the equation, and the concentration of the sample was  
198 calculated).

## 199 **2.10 Statistical analysis**

200 For statistical data analysis, GraphPad Prism 8.0 and SPSS 25.0 software were  
201 utilized. All studies were carried out three times, and the findings were reported as the  
202 mean standard deviation ( $\bar{x}\pm S$ ). When comparing two groups, the T test was  
203 employed, and when comparing multiple groups, the one-way ANOVA was utilized.  
204 The difference was statistically significant when  $P<0.05$  was used.

205

206

## **3 Result**

### 207 **3.1 16HBE cell activity after 24h exposure to PM<sub>2.5</sub> and PM<sub>2.5</sub>+O<sub>3</sub> complexes**

208 After 24h of contamination, the cellular activity of the PM<sub>2.5</sub> group was reduced  
209 ( $P<0.05$ ) compared with the control group, and the reduction of cellular activity was  
210 more obvious in the PM<sub>2.5</sub>+O<sub>3</sub> group ( $P<0.05$ ); the cellular activity of the PM<sub>2.5</sub>+O<sub>3</sub>



211 concentration group was decreased ( $P < 0.05$ ) compared with that of the PM<sub>2.5</sub>  
212 group (Figure 3.1).

### 213 **3.2 Inflammatory effects of 16HBE after 24h exposure to PM<sub>2.5</sub> and PM<sub>2.5</sub>+O<sub>3</sub>** 214 **composite exposure**

215 After 24 h of contamination, the expression of inflammatory factors IL-1 $\beta$  and  
216 IL-8 transcript and protein levels were elevated in the PM<sub>2.5</sub> group compared with  
217 the control group ( $P < 0.05$ ); the expression of inflammatory factors transcript and  
218 protein levels were more significantly elevated in the PM<sub>2.5</sub>+O<sub>3</sub> group ( $P < 0.05$ ); the  
219 expression of inflammatory factors IL-1 $\beta$  and IL-8 transcript and protein levels were  
220 elevated in the PM<sub>2.5</sub>+O<sub>3</sub> concentration group compared with the PM<sub>2.5</sub> group ( $P <$   
221  $0.05$ ). transcript and protein levels were elevated ( $P < 0.05$ ) (Figure 3.2).

### 222 **3.3 qRT-PCR validation of circRNAs associated with cellular inflammatory** 223 **effects**

224 Based on the high-throughput sequencing results, 10 differentially expressed  
225 circRNAs associated with cellular inflammatory pathways were screened out, and in  
226 order to verify the accuracy of the RNA-seq results, we performed qRT-PCR on these  
227 10 circRNAs again. Hsa\_circ\_0001495 expression level was consistent with the  
228 sequencing results, and hsa\_circ\_0001495 was identified as the target circRNA. After  
229 staining 16HBE cells with 0, PM<sub>2.5</sub> group, and PM<sub>2.5</sub>+O<sub>3</sub> composite exposure group,  
230 respectively, for 24 h, the hsa\_circ\_0007766 expression level was reduced in PM<sub>2.5</sub>  
231 group as well as in PM<sub>2.5</sub>+O<sub>3</sub> composite exposure group compared with the control  
232 group ( $P < 0.05$ ), and the PM<sub>2.5</sub>+O<sub>3</sub> composite exposure group had a more  
233 pronounced ( $P < 0.05$ ) reduction in hsa\_circ\_0001495 expression level was reduced in the  
234 PM<sub>2.5</sub>+O<sub>3</sub> compound exposure group compared with the PM<sub>2.5</sub> group ( $P < 0.05$ ). It  
235 indicates that hsa\_circ\_0001495 suppresses the inflammatory response in 16HBE  
236 cells. (Figure 3.3).

### 237 **3.4 RNase R digestive test**

238 After RNase R treatment, the expression of the endogenous ACTB was  
239 significantly reduced ( $P < 0.05$ ), whereas hsa\_circ\_0001495 was able to tolerate  
240 RNase R digestion, suggesting that hsa\_circ\_0001495 has a cyclic structure. (figure  
241 3.4)

### 242 **3.5 Nucleocytoplasmic separation experiment**

243 ACTB and U6 were mainly distributed in the cytoplasm and nucleus,  
244 respectively, indicating that the nucleoplasmic segregation experiment was successful,  
245 while hsa\_circ\_0001495 was mainly expressed in the cytoplasm. (figure 3.5)

### 246 **3.6 Fluorescence in situ hybridization experiment**

247 To further verify the distribution of hsa\_circ\_0001495 in cells, we localized  
248 hsa\_circ\_0001495 through fluorescence in situ hybridization experiment, and found  
249 that Cy3-labeled hsa\_circ\_0001495 was distributed in both nucleus and cytoplasm  
250 (Figure 3.6)

### 251 **3.7 hsa\_circ\_0001495 Overexpression effect**

252 Compared with the NC group, the hsa\_circ\_0007766 overexpression group was  
253 able to effectively increase the expression of hsa\_circ\_0007766 ( $P < 0.05$ ). (Figure 3.7)

### 254 **3.8 Hsa\_circ\_0001495 functional verification experiment**

255 The cellular inflammatory effect was elevated after PM2.5+O<sub>3</sub> complex  
256 exposure to 16HBE cells ( $P < 0.05$ ); compared to the NC group, the cellular  
257 inflammatory effect was decreased after overexpression of hsa\_circ\_0007766 ( $P <$   
258  $0.05$ ); compared to the NC+PM2.5 group, the cellular inflammation in the  
259 hsa\_circ\_0007766+PM2.5 group effect was decreased ( $P < 0.05$ ). Thus,  
260 overexpression of hsa\_circ\_0007766 decreased the cellular inflammatory effect,  
261 suggesting that hsa\_circ\_0007766 has an anti-inflammatory effect in 16HBE cell  
262 inflammation caused by PM2.5+O<sub>3</sub> compound exposure. (Figure 3.8)

263

264

## **4 Discussion**

265 According to the 2022 China Ecological Environment Status Bulletin, the  
266 average atmospheric PM<sub>2.5</sub> and O<sub>3</sub> concentrations in 339 cities at prefecture level  
267 and above in China were 29 µg/m<sup>3</sup> and 145 µg/m<sup>3</sup>, respectively, and the number of  
268 exceedance days in which PM<sub>2.5</sub> and O<sub>3</sub> were the primary pollutants accounted for  
269 36.9% and 47.9% of the total number of exceedance days, respectively; compared  
270 with 2021, the proportion of exceedance days of both PM<sub>2.5</sub> and O<sub>3</sub> increased, and  
271 the concentration of O<sub>3</sub> increased. Compared with 2021, the proportion of days with  
272 exceedance of atmospheric PM<sub>2.5</sub> and O<sub>3</sub> increased, and the concentration of O<sub>3</sub>  
273 increased. Short-term exposure to PM<sub>2.5</sub> and warm-season O<sub>3</sub> was significantly  
274 associated with an increased risk of mortality<sup>[19]</sup>, and the combined PM<sub>2.5</sub> and O<sub>3</sub>  
275 pollution has become a major air pollution problem in China. Many epidemiological  
276 evidences show that PM<sub>2.5</sub> is closely related to respiratory diseases, and the damage  
277 of fine particulate matter to the respiratory system has been confirmed in vivo and in  
278 vitro. The respiratory system is the main route of PM<sub>2.5</sub> inhalation<sup>[20]</sup> Current  
279 epidemiological data show a significant correlation between PM<sub>2.5</sub> and respiratory  
280 diseases . Long-term exposure to fine particulate matter (PM<sub>2.5</sub>) is associated with  
281 reduced lung function in adults<sup>[5, 21]</sup> .

282 The association between atmospheric O<sub>3</sub> pollution and increased risk of  
283 respiratory diseases is well established<sup>[6]</sup>. Inhalation of O<sub>3</sub> may damage lung  
284 epithelial cells<sup>[7, 8]</sup>. The results of Kim <sup>[22]</sup> and others have shown that long-term  
285 exposure to O<sub>3</sub> is associated with an increased risk of respiratory mortality. Long-  
286 term standards for O<sub>3</sub> and PM should be considered to protect the respiratory health  
287 of the general population and patients with chronic respiratory diseases.

288 Inflammation is a defence-based pathological response following an external  
289 stimulus, and excessive inflammation is considered to be the main causative event  
290 leading to the development or exacerbation of respiratory diseases <sup>[23]</sup>. The

291 inflammatory effect of PM<sub>2.5</sub> and O<sub>3</sub> on the respiratory system is one of their main  
292 toxic effects, and there is a synergistic effect between them. Numerous studies have  
293 shown that the inflammatory response is considered to be the underlying pathogenic  
294 mechanism in the mechanism of respiratory system damage caused by PM<sub>2.5</sub> and  
295 O<sub>3</sub>. Sokolowska<sup>[24]</sup> and others reviewed the latest data on the mechanisms of O<sub>3</sub>  
296 damage to different cell types and pathways, with a focus on the role of the IL-1  
297 family of cytokines and the related IL-33. It has been suggested <sup>[25]</sup> that the IL-33  
298 /ST2 pathway contributes to O<sub>3</sub>-induced airway hyperresponsiveness in male mice,  
299 and that the interaction of O<sub>3</sub> and traffic-associated PM<sub>2.5</sub> produces significantly more  
300 hydroxyl radicals than PM<sub>2.5</sub> alone, suggesting that combined exposure to PM<sub>2.5</sub> and  
301 O<sub>3</sub> is more likely to lead to organismal inflammation. Therefore, it is necessary to  
302 carry out compound exposure studies to provide an important scientific basis for the  
303 prevention and control of environmentally related diseases.

304 So far, although O<sub>3</sub> and PM<sub>2.5</sub>-induced respiratory inflammation has received  
305 much attention from many scholars, the molecular mechanism of compound exposure  
306 is still unclear, and there is an urgent need to find new ways to explore. A large  
307 number of circRNAs have been found to regulate gene expression and play important  
308 biological functions. circRNAs play an important role in body inflammation.  
309 Therefore, we explored the role of circRNAs in the inflammatory effects caused by O<sub>3</sub>  
310 and PM<sub>2.5</sub> exposure in vitro, aiming to provide gene therapy targets for O<sub>3</sub> and PM<sub>2.5</sub>-  
311 induced inflammation at the level of non-coding RNAs, and to expand a new direction  
312 for the study of inflammatory mechanisms.

313 In this study, we identified for the first time the relationship between  
314 hsa\_circ\_0007766 and the inflammatory response of 16HBE cells induced by the  
315 combined exposure of PM<sub>2.5</sub> and O<sub>3</sub>. hsa\_circ\_0007766 was abnormally low  
316 expressed in the inflammatory cells, revealing its biological function as an inhibitor of

317 inflammation in the inflammatory response of 16HBE cells induced by the combined  
318 exposure of PM<sub>2.5</sub> and O<sub>3</sub>. These findings provide new ideas and directions for the  
319 search of diagnostic and therapeutic targets for inflammation induced by the  
320 combined exposure of PM<sub>2.5</sub> and O<sub>3</sub>.

321

322

## Acknowledgements

323 This work was supported by the National Natural Science Foundation of  
324 China(Grant no.21477045),the National Key Research and Development Program of  
325 China (No.2023YFC39005204),the Central Public-Interest Scientific Institution Basal  
326 Research Fund (Grant no.PM-zx703-202004-155,Grant no.PM-zx703-202204-164) .

327

328

## References

- 329 [1] Schweizer D, Cisneros R, Traina S, et al. Using National Ambient Air Quality  
330 Standards for fine particulate matter to assess regional wildland fire smoke  
331 and air quality management [J]. *Journal of environmental management*, 2017,  
332 201: 345-56.
- 333 [2] Matsui H, Mahowald NM, Moteki N, et al. Anthropogenic combustion iron as  
334 a complex climate forcer [J]. *Nature communications*, 2018, 9(1): 1593.
- 335 [3] Shang Y, Sun Z, Cao J, et al. Systematic review of Chinese studies of short-  
336 term exposure to air pollution and daily mortality [J]. *Environment*  
337 *international*, 2013, 54: 100-11.
- 338 [4] Bell ML, Mcdermott A, Zeger SL, et al. Ozone and short-term mortality in 95  
339 US urban communities, 1987-2000 [J]. *Jama*, 2004, 292(19): 2372-8.
- 340 [5] Medina-Ramón M, Zanobetti A, Schwartz J. The effect of ozone and PM10 on  
341 hospital admissions for pneumonia and chronic obstructive pulmonary disease:  
342 a national multicity study [J]. *American journal of epidemiology*, 2006, 163(6):  
343 579-88.
- 344 [6] Malig BJ, Pearson DL, Chang YB, et al. A Time-Stratified Case-Crossover

- 345 Study of Ambient Ozone Exposure and Emergency Department Visits for  
346 Specific Respiratory Diagnoses in California (2005-2008) [J]. *Environmental*  
347 *health perspectives*, 2016, 124(6): 745-53.
- 348 [7] Lagerkvist BJ, Bernard A, Blomberg A, et al. Pulmonary epithelial integrity in  
349 children: relationship to ambient ozone exposure and swimming pool  
350 attendance [J]. *Environmental health perspectives*, 2004, 112(17): 1768-71.
- 351 [8] Blomberg A, Mudway I, Svensson M, et al. Clara cell protein as a biomarker  
352 for ozone-induced lung injury in humans [J]. *The European respiratory journal*,  
353 2003, 22(6): 883-8.
- 354 [9] Wong EM, Walby WF, Wilson DW, et al. Ultrafine Particulate Matter  
355 Combined With Ozone Exacerbates Lung Injury in Mature Adult Rats With  
356 Cardiovascular Disease [J]. *Toxicological sciences : an official journal of the*  
357 *Society of Toxicology*, 2018, 163(1): 140-51.
- 358 [10] Happonen MS, Salonen RO, Hälinen AI, et al. Inflammation and tissue damage in  
359 mouse lung by single and repeated dosing of urban air coarse and fine  
360 particles collected from six European cities [J]. *Inhalation toxicology*, 2010,  
361 22(5): 402-16.
- 362 [11] Michaudel C, Maillet I, Fauconnier L, et al. Interleukin-1 $\alpha$  Mediates Ozone-  
363 Induced Myeloid Differentiation Factor-88-Dependent Epithelial Tissue Injury  
364 and Inflammation [J]. *Frontiers in immunology*, 2018, 9: 916.
- 365 [12] Zhang HD, Jiang LH, Sun DW, et al. CircRNA: a novel type of biomarker for  
366 cancer [J]. *Breast cancer (Tokyo, Japan)*, 2018, 25(1): 1-7.
- 367 [13] Hong J, Tan Y, Wang Y, et al. Mechanism of Interaction between  
368 hsa\_circ\_0002854 and MAPK1 Protein in PM(2.5)-Induced Apoptosis of  
369 Human Bronchial Epithelial Cells [J]. *Toxics*, 2023, 11(11).
- 370 [14] Tan Y, Wang Y, Zou Y, et al. LncRNA LOC101927514 regulates PM(2.5)-  
371 driven inflammation in human bronchial epithelial cells through binding p-  
372 STAT3 protein [J]. *Toxicology letters*, 2020, 319: 119-28.
- 373 [15] Xu Z, Wu H, Zhang H, et al. Interleukins 6/8 and cyclooxygenase-2 release  
374 and expressions are regulated by oxidative stress-JAK2/STAT3 signaling

- 375 pathway in human bronchial epithelial cells exposed to particulate matter  $\leq 2.5$   
376  $\mu\text{m}$  [J]. *Journal of applied toxicology : JAT*, 2020, 40(9): 1210-8.
- 377 [16] Chen QZ, Zhou YB, Zhou LF, et al. TRPC6 modulates adhesion of neutrophils  
378 to airway epithelial cells via NF- $\kappa$ B activation and ICAM-1 expression with  
379 ozone exposure [J]. *Experimental cell research*, 2019, 377(1-2): 56-66.
- 380 [17] Poma A, Colafarina S, Aruffo E, et al. Effects of ozone exposure on human  
381 epithelial adenocarcinoma and normal fibroblasts cells [J]. *PloS one*, 2017,  
382 12(9): e0184519.
- 383 [18] Zhao X, Li Y, Lin X, et al. Ozone induces autophagy in rat chondrocytes  
384 stimulated with IL-1 $\beta$  through the AMPK/mTOR signaling pathway [J].  
385 *Journal of pain research*, 2018, 11: 3003-17.
- 386 [19] Di Q, Dai L, Wang Y, et al. Association of Short-term Exposure to Air  
387 Pollution With Mortality in Older Adults [J]. *Jama*, 2017, 318(24): 2446-56.
- 388 [20] Yang L, Li C, Tang X. The Impact of PM(2.5) on the Host Defense of  
389 Respiratory System [J]. *Frontiers in cell and developmental biology*, 2020, 8:  
390 91.
- 391 [21] Rice MB, Ljungman PL, Wilker EH, et al. Long-term exposure to traffic  
392 emissions and fine particulate matter and lung function decline in the  
393 Framingham heart study [J]. *American journal of respiratory and critical care*  
394 *medicine*, 2015, 191(6): 656-64.
- 395 [22] Kim SY, Kim E, Kim WJ. Health Effects of Ozone on Respiratory Diseases [J].  
396 *Tuberculosis and respiratory diseases*, 2020, 83(Supple 1): S6-s11.
- 397 [23] Guo C, Lv S, Liu Y, et al. Biomarkers for the adverse effects on respiratory  
398 system health associated with atmospheric particulate matter exposure [J].  
399 *Journal of hazardous materials*, 2022, 421: 126760.
- 400 [24] Sokolowska M, Quesniaux VFJ, Akdis CA, et al. Acute Respiratory Barrier  
401 Disruption by Ozone Exposure in Mice [J]. *Frontiers in immunology*, 2019, 10:  
402 2169.
- 403 [25] Valavanidis A, Loridas S, Vlahogianni T, et al. Influence of ozone on traffic-  
404 related particulate matter on the generation of hydroxyl radicals through a

405 heterogeneous synergistic effect [J]. Journal of hazardous materials, 2009,  
406 162(2-3): 886-92.

407

408

## Tables

409 TableS1 circRNA primer sequence list

410 TableS2 FISH probe sequence

411

412

## Figure captions

413 Figure 3.1 Effect of PM2.5 and PM2.5+O3 staining on the viability of 16HBE cells  
414 after 24h of poisoning

415 Figure 3.2 Transcription and protein expression levels of cellular inflammatory factors  
416 IL-1 $\beta$  and IL-8 after 24 h of PM2.5 and PM2.5+O3 stimulation

417 Figure 3.3 mRNA transcript levels of circRNAs in PM2.5 and PM2.5+O3-stained  
418 16HBE cells after 24h

419 Figure 3.4 RNaseR digestion experiment

420 Figure 3.5 Nucleocytoplasmic separation experiment

421 Figure 3.6 Fluorescence in situ hybridization experiment

422 Figure 3.7 Hsa\_circ\_0001495 Overexpression effect

423 Figure 3.8 Transcription and protein expression levels of IL-1 $\beta$ , IL-8 after  
424 overexpression of hsa\_circ\_0007766 or combined exposure to PM2.5+O3



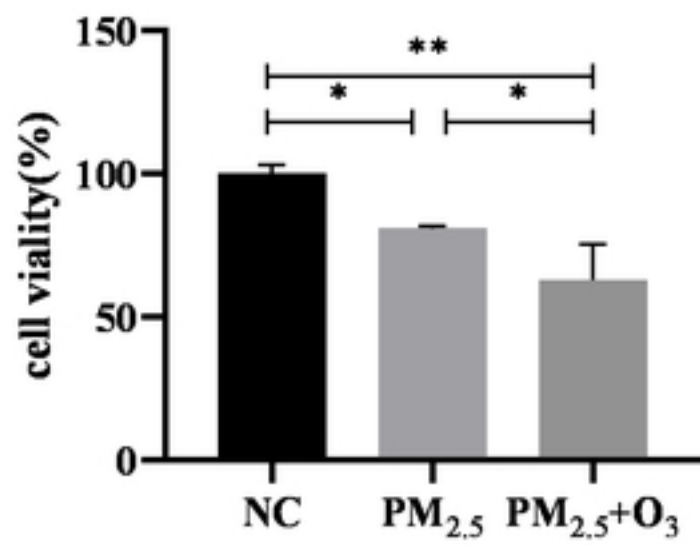


Figure 3.1 Effect of PM<sub>2.5</sub> and PM<sub>2.5</sub>+O<sub>3</sub> staining on the viability of 16HBE cells after 24h of poisoning

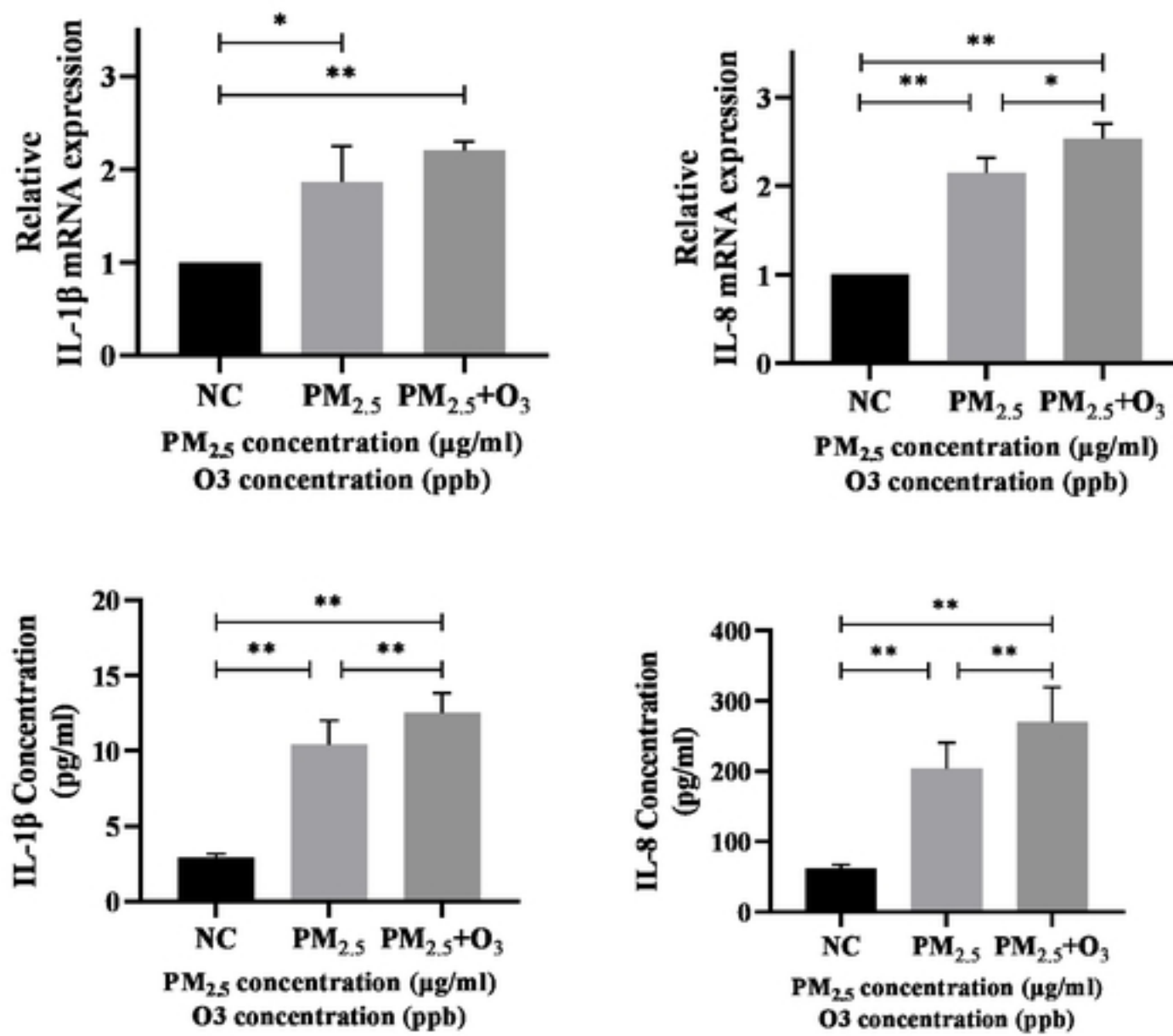


Figure 3.2 Transcription and protein expression levels of cellular inflammatory factors IL-1β and IL-8 after 24 h of PM<sub>2.5</sub> and PM<sub>2.5</sub>+O<sub>3</sub> stimulation

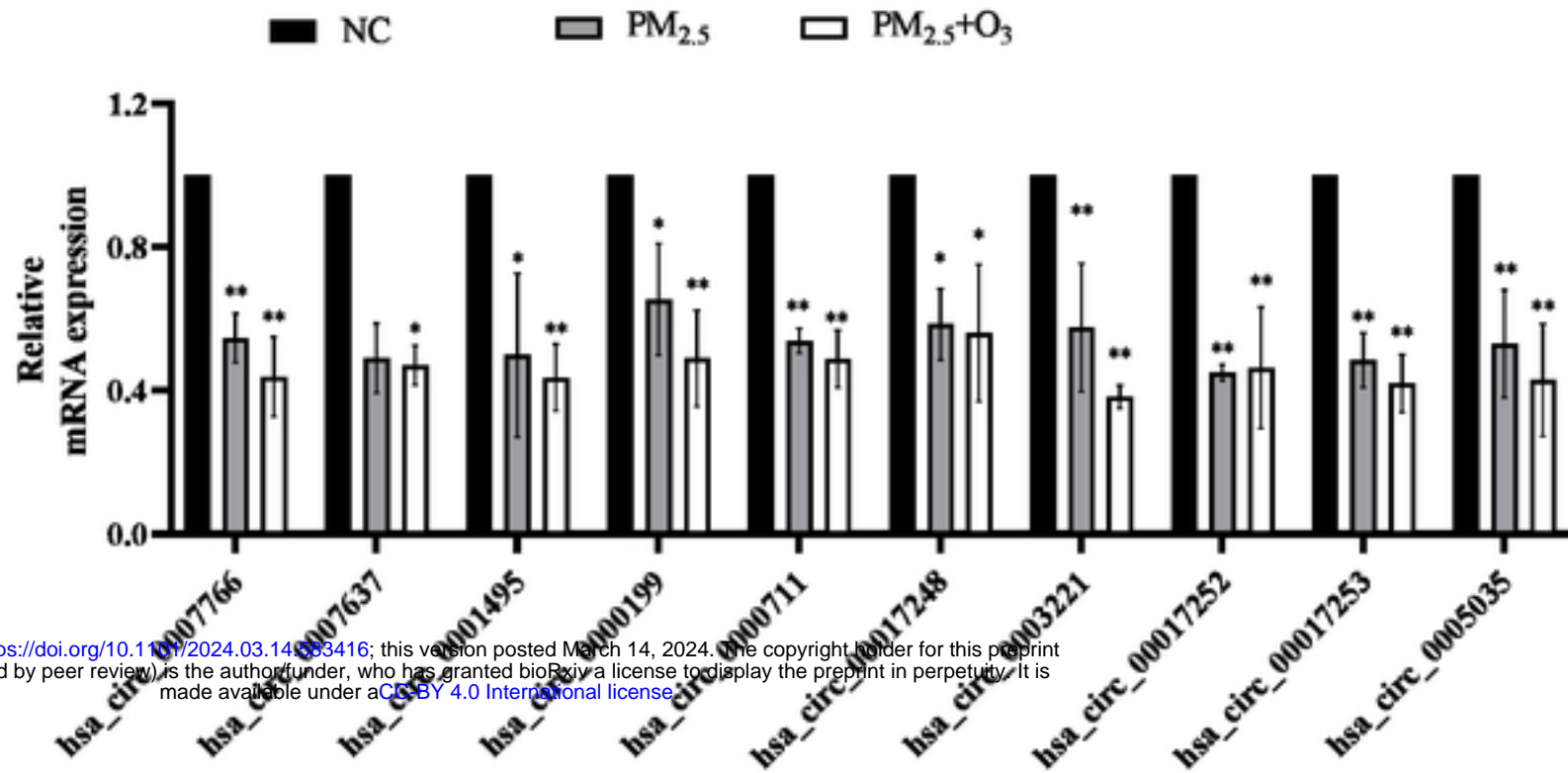


Figure 3.3 mRNA transcript levels of circRNAs in PM<sub>2.5</sub> and PM<sub>2.5</sub>+O<sub>3</sub>-stained 16HBE cells after 24h

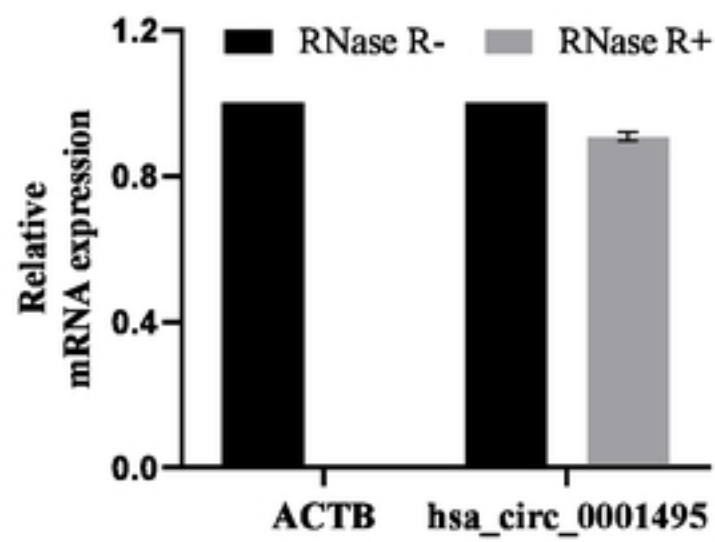
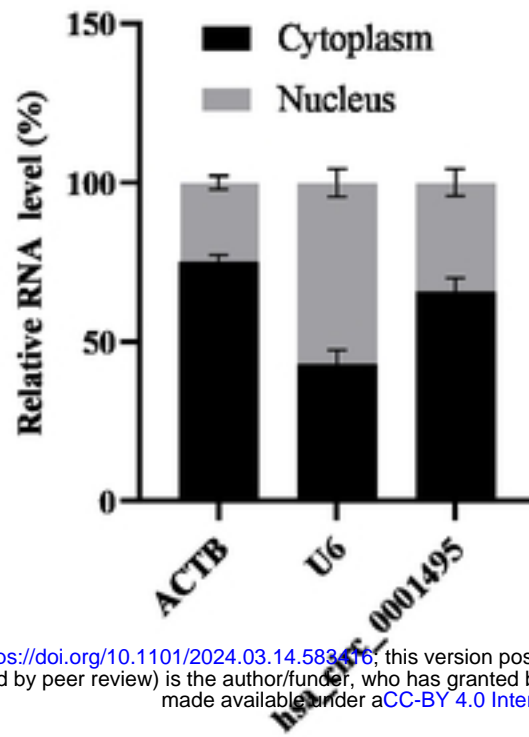


Figure 3.4 RNaseR digestion experiment



bioRxiv preprint doi: <https://doi.org/10.1101/2024.03.14.583176>; this version posted March 14, 2024. The copyright holder for this preprint (which was not certified by peer review) is the author/funder, who has granted bioRxiv a license to display the preprint in perpetuity. It is made available under aCC-BY 4.0 International license.

Figure 3.5 Nucleocytoplasmic separation experiment

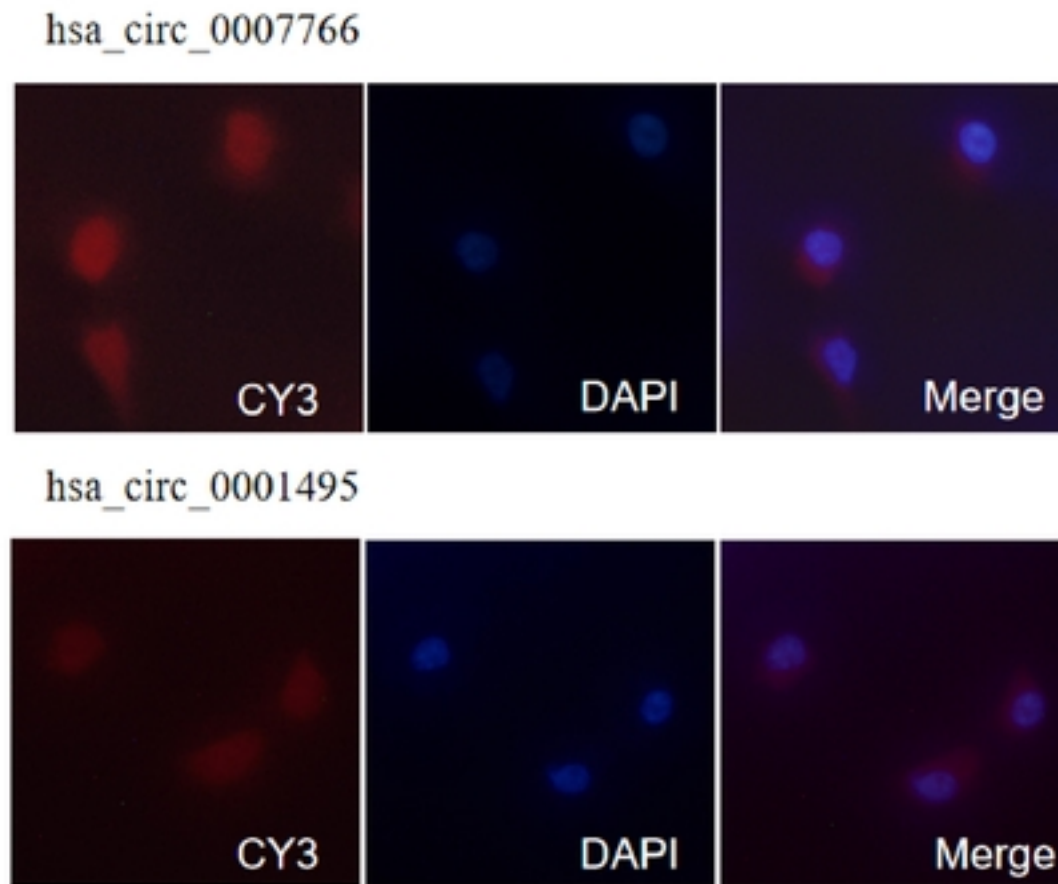


Figure 3.6 Fluorescence in situ hybridization experiment

bioRxiv preprint doi: <https://doi.org/10.1101/2024.03.14.583416>; this version posted March 14, 2024. The copyright holder for this preprint (which was not certified by peer review) is the author/funder, who has granted bioRxiv a license to display the preprint in perpetuity. It is made available under aCC-BY 4.0 International license.

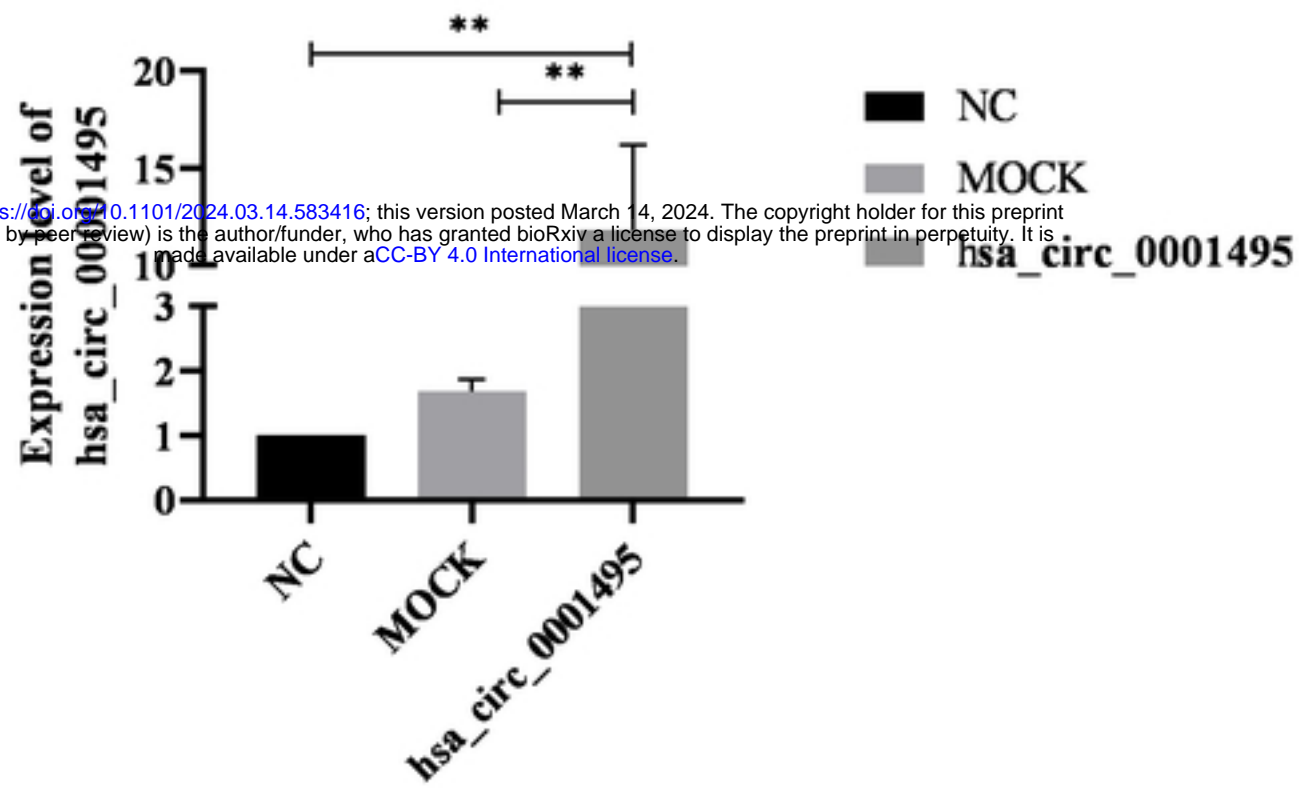
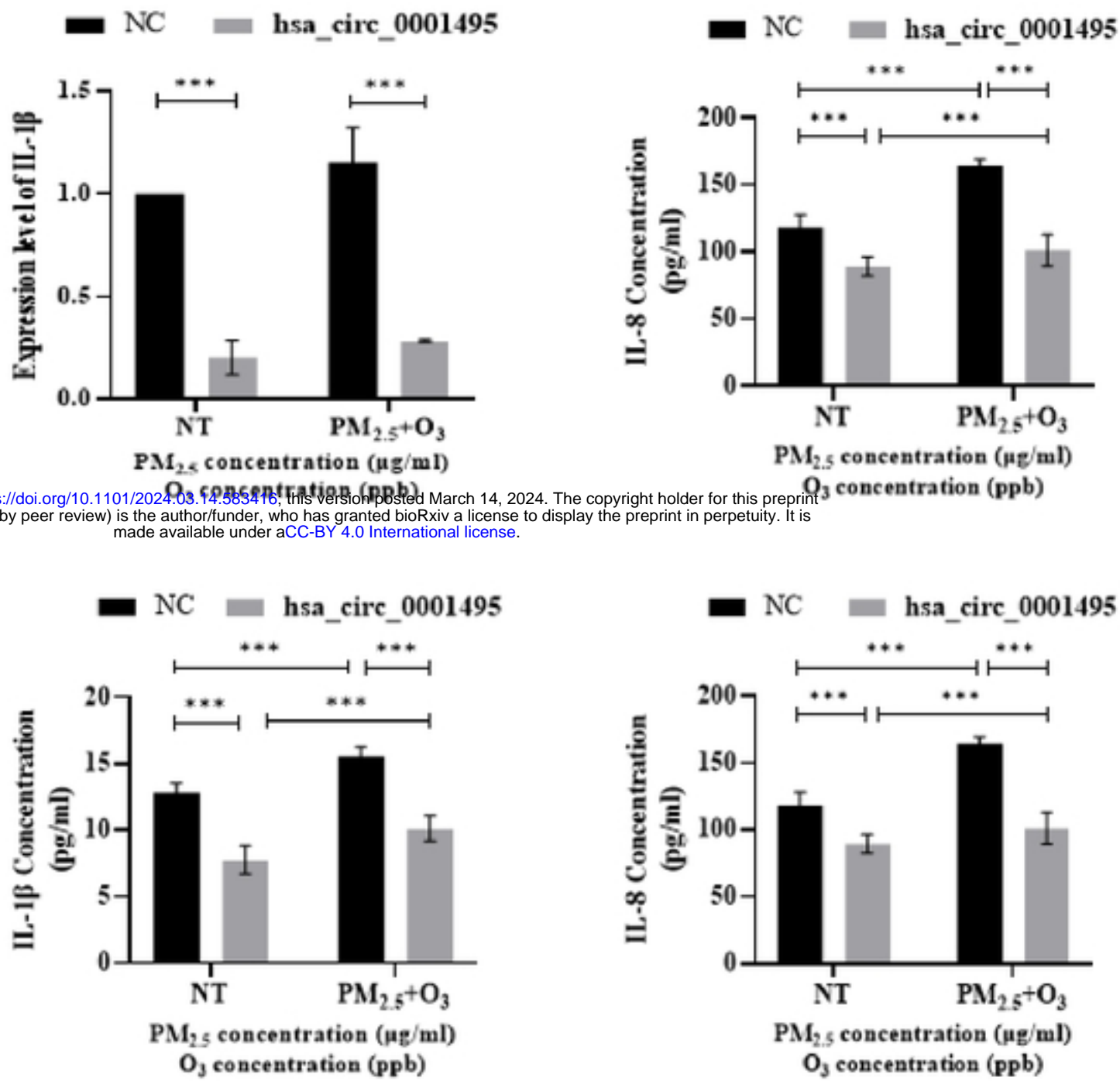


Figure 3.7 Hsa\_circ\_0001495 Overexpression effect



bioRxiv preprint doi: <https://doi.org/10.1101/2024.03.14.583416>; this version posted March 14, 2024. The copyright holder for this preprint (which was not certified by peer review) is the author/funder, who has granted bioRxiv a license to display the preprint in perpetuity. It is made available under aCC-BY 4.0 International license.

Figure 3.8 Transcription and protein expression levels of IL-1 $\beta$ , IL-8 after overexpression of hsa\_circ\_0007766 or combined exposure to PM<sub>2.5</sub>+O<sub>3</sub>

Table S1 circRNA primer sequence list

引物名称	引物序列(5' to 3')
hsa_circ_0007766-F	TGTGTGACTGCCTGTCCCTG
hsa_circ_0007766-R	AATCCGCAGCCTCTGCAGTG
hsa_circ_0007637-F	AGGAGGCATGGCCAAGATT
hsa_circ_0007637-R	TTGATACTAGAGCCGCTGCC
hsa_circ_0001495-F	ATGGTGAATGGAATAATTGTGTGCC
hsa_circ_0001495-R	ATTCCATCTGTCTGATTTGGTGCT
hsa_circ_0000199-F	CAAATAAACGCCTTGGTGGA
hsa_circ_0000199-R	ATAGAAACGTGTGCGGTCCT
hsa_circ_0000711-F	CACTAGACTGGCCTTTACC

hsa_circ_0000711-R	CACAATCATCTGGCTCAA
hsa_circ_0017248-F	AGGACCGCACACGTTTCTAT
hsa_circ_0017248-R	AGGGTTTGGATTCTCTGCTG
hsa_circ_0003221-F	GGCGATCATACTGGGAGATG
hsa_circ_0003221-R	TGTGATTCAAGTTGGGGTCA
hsa_circ_0017252-F	CCTCCAGACAAAAGACCGT
hsa_circ_0017252-R	CCCCAACTTGGAGAAATGGT
hsa_circ_0017253-F	TGGTTCGAGAGAAGGCAAGT
hsa_circ_0017253-R	GGTTTGGATTCTCTGCTGCT
hsa_circ_0005035-F	CAAACCGCTGCCAGAAAATCT
hsa_circ_0005035-R	ACTCGGTAATGACCGTGAGC
ACTB-F	CCCTGCCAGCAACTACCA
ACTB-R	TGTTGCCAGCCTCCTTCTCT
IL-1 $\beta$ -F	ACTCCATGGCTCTGGTGCTC
IL-1 $\beta$ -R	ATGGCAACTCCCAGTGGTGG
IL-8-F	GGGAAGAAAGAAGCAAGAATGGTGT
IL-8-R	TGTATGGGTGACGCAGAGCT
U6-F	CTCGCTTCGGCAGCACA
U6-R	AACGCTTCACGAATTTGCGT

bioRxiv preprint doi: <https://doi.org/10.1101/2024.03.14.583416>; this version posted March 14, 2024. The copyright holder for this preprint (which was not certified by peer review) is the author/funder, who has granted bioRxiv a license to display the preprint in perpetuity. It is made available under aCC-BY 4.0 International license.

TableS2 FISH probe sequence

基因名称	探针序列(5'-3')	修饰方式
hsa_circ_0007766 probe	CACCTCCTGGATATCAGGGACAGGCAG+TCAC	5'CY3
hsa_circ_0001495 probe	CCATTCACCATTATCTGGGCACACAATTATT	5'CY3

> hsa\_circ\_0001495 overexpression sequence

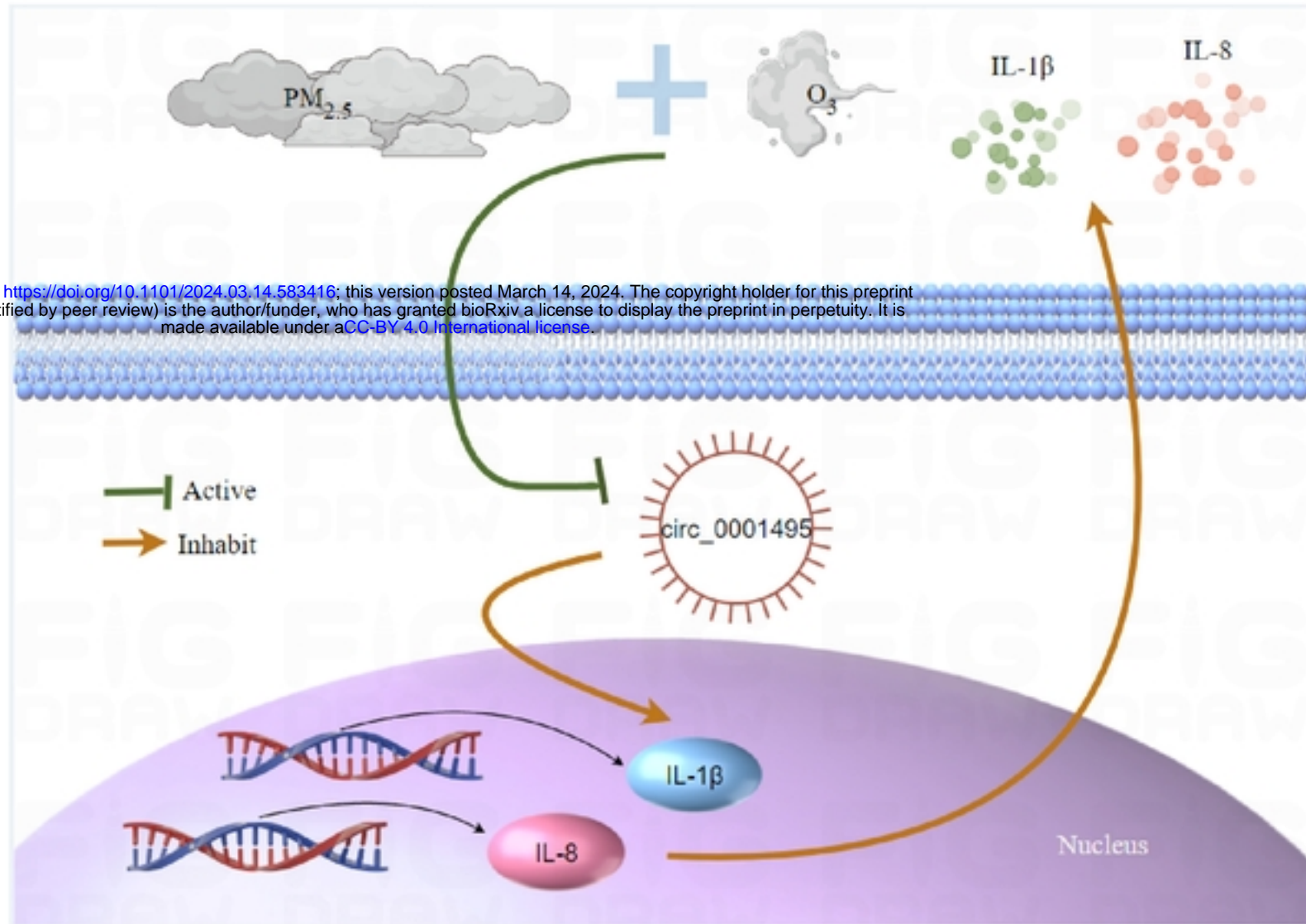
```

agtagagacgggggttcaccatgttgccaggctggtcttCACTTTTTGTAAAGGTACGTAATAAT
GACTTTTTTTTTTATACTTCAGAATAATTGTGTGCCCAAGAAGATGCTGCAG
CTGGTTGGTGTCACTGCCATGTTTATTGCAAGCAAATATGAAGAAATGTAC
CCTCCAGAAATTGGTGACTTTGCTTTTGTGACTGACAACACTTATACTAAG
CACCAAATCAGACAGATGGAAATGAAGATTCTAAGAGCTTTAAACTTTGG
TCTGGGTCGGCCTCTACCTTTGCACTTCCTTCGGAGAGCATCTAAGATTGG
AGAGGTTGATGTCGAGCAACATACTTTGGCCAAATACCTGATGGAACTAA

```

CTATGTTGGACTATGACATGGTGCACCTTTCCTCCTTCTCAAATTGCAGCAG  
GAGCTTTTTGCTTAGCACTGAAAATTCTGGATAATGGTGAATGGGTAAGA  
AGCAAGGAAAAGAATTAgagaccagcctggccaacatggtgaaacctgtcttact

bioRxiv preprint doi: <https://doi.org/10.1101/2024.03.14.583416>; this version posted March 14, 2024. The copyright holder for this preprint (which was not certified by peer review) is the author/funder, who has granted bioRxiv a license to display the preprint in perpetuity. It is made available under aCC-BY 4.0 International license.



Graphical Abstract